PHYSICAL REVIEW E **75**, 050403(R) (2007)

Dynamic consequences of the fractal network of nanotube-poly(ethylene oxide) nanocomposites

Tirtha Chatterjee and Ramanan Krishnamoorti
Department of Chemical and Biomolecular Engineering, University of Houston, Houston, Texas 77204-4004, USA
(Received 10 December 2006; published 16 May 2007)

Dispersions of single walled carbon nanotubes (SWNTs), with an effective aspect ratio of ~650, in poly(ethylene oxide) (PEO) form fractal superstructures above their geometrical percolation and display rheological properties that follow time-temperature-composition-strain superpositioning. The concentration dependences of the elastic modulus of the network and the onset-strain for shear thinning are consistent with the short-range nature of the interactions that dominate these dispersions. The strain dependence of the damping behavior for the nanocomposites shows concentration invariance when represented against the local strain experienced by the network element, with the onset occurring at a local strain value of 0.1, similar to other nanocomposite systems dominated by weak interactions.

DOI: 10.1103/PhysRevE.75.050403 PACS number(s): 83.80.Hj, 61.43.Hv, 82.70.−y, 83.60.Bc

Dispersions of nanoparticles, especially anisotropic ones, in polymers offer significant potential for providing a wealth of attractive material properties [1,2]. Nevertheless, in spite of favorable thermodynamic driving forces for the creation of well-dispersed systems [3,4], the eventual realization of many of these dispersions is prevented even at modest volume fractions of the nanoparticles presumably due to the high aspect ratio and attractive interparticle interactions. The small strain viscoelastic response of such suspensions of dispersed nanoparticles [5–8], above a percolation threshold, display characteristics of gelation or jammed systems, similar to those demonstrated by more familiar colloidal suspensions [9,10]. For colloidal suspensions it has been shown previously that the linear elastic modulus of the gelled system and the onset of shear thinning are closely related to the interactions between the nanoparticles and the fractal structure of the gel-like material [11–13]. In this work we extend the work to fractal networks of single walled carbon nanotubes in a polymer matrix and demonstrate that the linear viscoelastic behavior is consistent with the weak attractive interactions between nanotubes. Further, we demonstrate that the concept of "time-temperature-composition" superposition valid for linear viscoelastic properties [13] can be extended to include the *nonlinear* response with a composition independent scaling behavior for the damping coefficient, indicating that the breakdown of the fractal network is also self-similar. Interestingly, computing the local strain based on a simple stress-distribution model indicates that the shear thinning for these and other weakly interacting systems, such as organoclay-polymer nanocomposites, is superposable with local strain.

The linear melt-state viscoelastic properties of the nanocomposites are examined using a combination of stress relaxation and small amplitude dynamic oscillatory shear. The linear stress relaxation data [Fig. 1(a)] indicate that for the nanocomposites with $p \geq 0.3$ vol. % there is no terminal liquidlike response for times as large as 4000 s with the modulus at long times for the 1 vol. % sample exceeding 10^5 dynes/cm^2. In this context, the relaxation time for the polymer is <0.01 s. Using a two point collocation method [14]

$$G(t) = G'(\omega) - 0.4G''(\omega) + 0.014G''(10\omega)\big|_{\omega=1/t} \quad (1)$$

and previously shown to be applicable for other polymer nanocomposites [6], we compare the linear stress relaxation measurements reported here [$G(t)$] with linear dynamic measurements (G' and G''). As seen in Fig. 1(a), the linear $G(t)$ data are in quantitative agreement with the corresponding linear dynamic viscoelastic properties. We note the similarity of the time dependence of the stress relaxation data for the samples with varying nanotube concentration and consider the possibility of creating time-composition master-curves for the linear viscoelastic data. In this context, an examination of the frequency dependence of the loss tangent

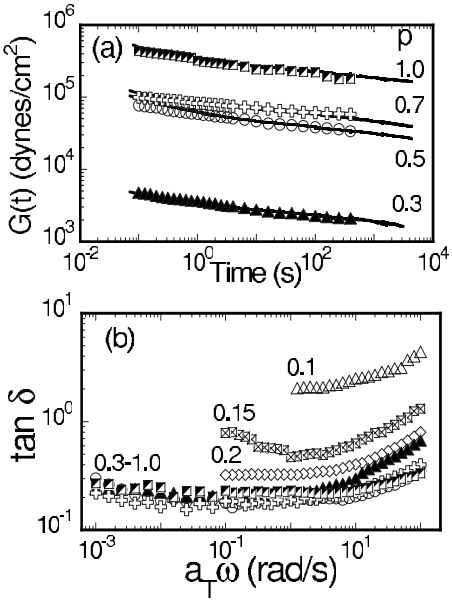

FIG. 1. (a) Comparison of the measured linear stress-relaxation modulus [$G(t)$] (solid line) and those calculated using Eq. (1) and linear dynamic measurements (symbols). For the nanocomposites with $p \geq 0.3$ (with p is vol% SWNT), a solid like behavior is observed. (b) Frequency dependence of the phase angle (tan δ) from linear dynamic oscillatory measurements. For $p \geq 0.3$, a composition invariant behavior is observed at low frequencies.

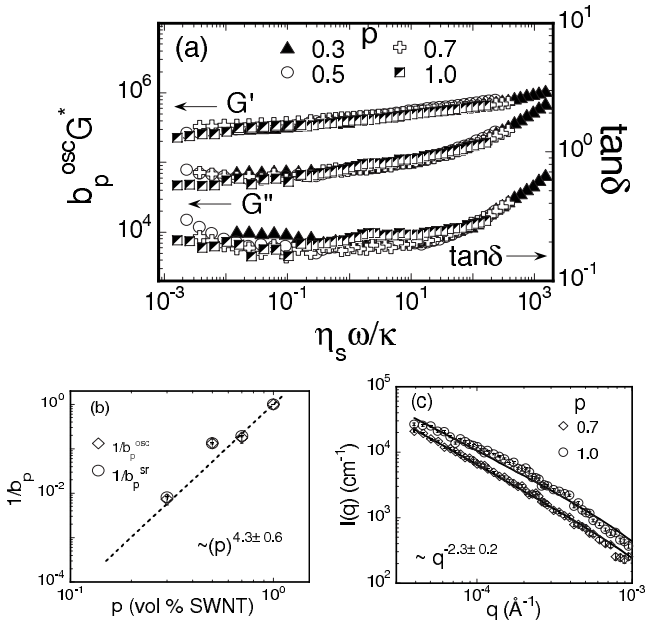

FIG. 2. (a) Time-temperature-composition superposed mastercurves for different linear dynamic rheological properties. (b) Modulus scaling factors used to obtain the composition superposition as a function of p. Consistent with the data in Fig. 1, the shift factors for the oscillatory and stress relaxation measurements are identical. (c) Wave vector (q) dependence of the ultra small angle neutron scattering intensities $I(q)$ for two nanocomposites. The data were obtained on BT5 instrument at NIST and reduced using standard methods [32]. The fits of the data to a power-law, smeared for experimental resolution and wavelength spread, are shown.

(tan $\delta=G''/G'$) shown in Fig. 1(b), is remarkably insightful. For the nanocomposites with $p/p_c \geqslant 3$ (p_c is the percolation threshold and ~0.09 vol. %) [15], the values of tan δ at low frequencies become independent of p and this suggests that the viscoelastic parameters can be superposed to form time-temperature-composition mastercurves, similar to those observed previously [13,16,17] [Fig. 2(a)]. Superpositioning clearly fails for concentrations only slightly above p_c [non-superposable tan δ values in Fig. 1(b)] and works well only for systems far above p_c ($p/p_c > 3$).

These mastercurves were developed by the application of both time and/or frequency and modulus shift factors comparable to previous efforts [13,16,17]. The shifts along the time axis were performed by superpositioning of tan δ data, while the shifts along the modulus axis were obtained by examination of the components of the complex viscosity. The superpositioning of viscosity was only dependent on the modulus shift factors and that of tan δ only dependent on the time shift factors. Nevertheless, the time shift factors (κ) were smaller than the modulus shift factors and yet proportional to the modulus shift factors as expected from theoretical considerations [13]. The modulus shift factors used to obtain mastercurves for the linear dynamic oscillatory shear data (b_p^{osc}) and for the linear stress relaxation data (b_p^{sr}) are comparable as seen in the Fig. 2(b).

Our results cover a relatively narrow range of frequency from being able to superpose viscoelastic data over a narrow composition range ($3 \leqslant p/p_c \leqslant 10$). For nanocomposites just above p_c, superpositioning fails because of a combination of the competing magnitudes of the viscoelasticity of the polymer and the fractal network and the changing nature of the nanotube network superstructure at concentrations close to p_c. On the other hand, at high concentrations the dispersed anisotropic nanotubes ($\alpha=L/D\sim650$) [15] are expected to have a large Onsager potential [10] [$U_0=(8/\pi)\times(L/D)\times(p/100)=16.5$ for $p=1.0$ vol. %] and thus form nematically ordered structures and not allowing for a comparison with the fractal networks. Further, for high nanotube loading samples, alignment of the nanotubes in response to the handling (compressive strains, etc.) becomes a significant experimental issue and disorientation in such nanocomposites is known to be extremely slow [18].

The linear viscoelastic data, for nanocomposites with $p \gg p_c$, are representative of a solidlike material and indicate that the superstructure of the nanotube dominates the viscoelastic response, as has been observed in general for soft-glassy materials [19,20]. The superpositioning of the linear viscoelastic response with composition indicates that the superstructure responsible for the dominant viscoelastic behavior in these nanocomposites is self-similar. This conjecture is verified using ultra small angle neutron scattering [Fig. 2(c)], where a fractal dimension (d_f)$=2.3\pm0.2$ is observed. This fractal dimension is consistent with previous observations of Hobbie and Fry [16] for multi walled carbon nanotubes (MWNTs) networks in polyisobutylene (PIB) and the simulation study reported by Ganesan *et al.* [21] for polymer bridged gels. Finally, the elastic strength (G_p) of this self-similar network superstructure measured as $1/b_p$ scales as $(p)^{4.3\pm0.6}$. The large value of the exponent is consistent with previous experiments observing elastic percolation in three dimensions [11–13], although somewhat lower than the values obtained for MWNT dispersions [16], and indicative of the significant increase in the network elasticity with added connections or bonds to the percolative network.

A study of the strain dependence of the viscoelastic response for the nanocomposites helps to elucidate further the fractal nature of the SWNT network. Specifically, the strain amplitude (γ_0) dependence of stress relaxation is shown in Fig. 3(a) for $p=0.7$. The trends observed there are typical for the series examined and briefly summarized as: (a) there is a linear regime that occurs at relatively low γ_0 values where the $G(t)$ data are independent of γ_0; (b) increasing the strain beyond the linear region ($\gamma_{critical}=0.003$ for $p=0.7$ vol. %) leads to a strain-softening behavior with conservation of the relaxation spectrum and suggesting the possibility of applying time-strain separability for these data [i.e., $G(t,\gamma)=h(\gamma)G(t)$, where $h(\gamma)$ is the damping function]; and (c) application of higher strain amplitude ($\gamma_0 \geqslant 0.08\pm0.02$ for $p=0.7$), the relaxation spectrum is no longer conserved and time-strain superposability is no longer valid.

The value of $\gamma_{critical}$ decreases with increasing p [Fig. 3(b)] and suggests that with increased nanotube loading the structural transformations to the nanotube superstructure occur at progressively smaller deformations. The damping function $h(\gamma)$ also superposes somewhat reasonably, as shown in Fig. 4(a), by normalizing the bulk strain γ bulk by

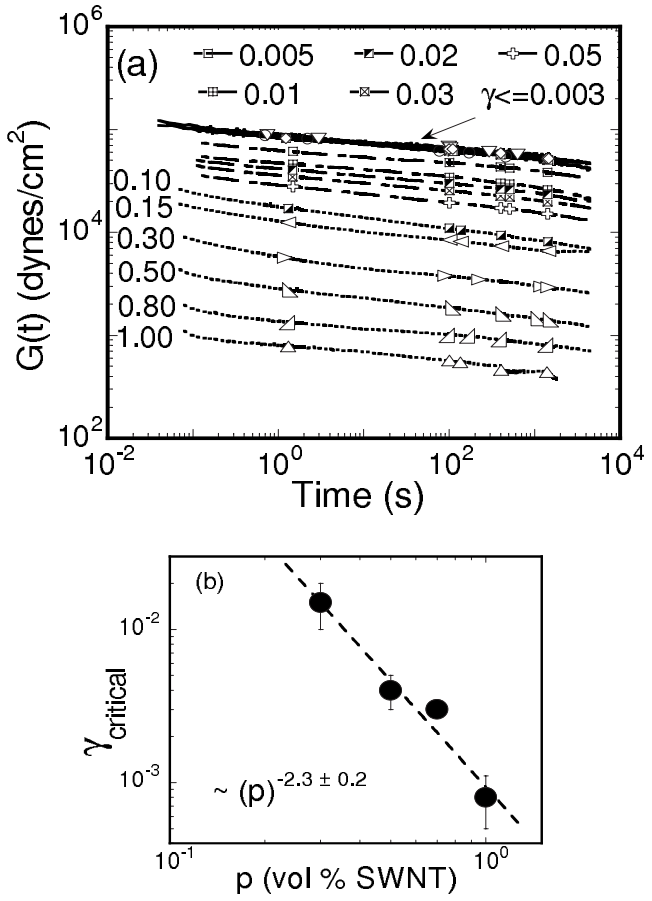

FIG. 3. (a) Representative stress relaxation behavior ($p=0.7$) as a function of the applied (bulk) strain amplitude. For low-amplitude strain, linear behavior is observed followed by a time-strain superposable zone. At higher strain amplitude, time-strain superposability is violated. (b) The composition dependence of the critical strain for the onset of shear thinning is shown; the scaling behavior is consistent with the short range interactions dominating these nanocomposites.

γ_{critical}; raising the possibility that the nature of shear-thinning is perhaps self-similar in these nanocomposite materials. Further, γ_{critical} scales as $(p)^{-2.3\pm0.2}$ and suggests that the intertube interactions and the multiple connections between percolating networks dominate the onset of shear thinning. This scaling of γ_{critical} and the previously demonstrated strong scaling of the elastic modulus is typical of fractal networks such as those of colloidal gels [12], layered silicate [18], flocculated silica spheres [22] and multiwalled carbon nanotube dispersions [16] which with increasing mass become stiffer and more fragile. Similar scaling is anticipated from theoretical efforts [23,24] examining the three-dimensional percolation of random percolating elements and from computer simulations [25,26] considering individual bonds resist both bending and stretching (i.e., enthalpic networks [21]).

Specifically, using the development of Shih *et al.* [12] for fractal networks with $p \gg p_c$, where the interactions between flocs dominate over those within a floc (the strong link regime) we can evaluate the nature of the fractal network in these nanocomposites. Such a modeling is prompted by our

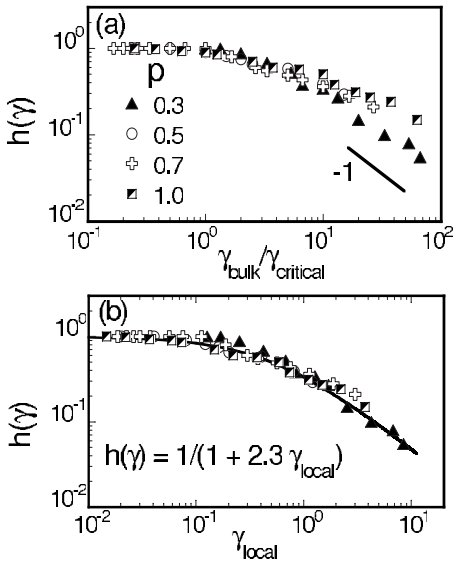

FIG. 4. (a) Damping function $h(\gamma)$ required for time-strain superposition is plotted against a reduced strain ($\gamma_{\text{bulk}}/\gamma_{\text{critical}}$). (b) The local strain [Eq. (2)] dependence of $h(\gamma)$. The onset of the shear thinning is observed at $\gamma_{\text{local}} \sim 0.1$ and is similar to other nanocomposite systems with short-range interactions.

observation of fractal-like scattering behavior observed for these dispersions. It is anticipated that the scaling for the elasticity (G_p) and critical strain (γ_{critical}) follow p^{μ} and $p^{-\delta}$ respectively with $\mu=(D+d_b)/(D-d_f)$ and $\delta=(1+d_b)/(D-d_f)$, where d_b and d_f are the backbone and fractal dimensions of the network and D is the Euclidian dimension. From the observed values of $\mu=4.3\pm0.6$ and $\delta=2.3\pm0.2$ for the nanotube based systems, we calculate the backbone and fractal dimensions of the network to be $d_b=1.1\pm0.2$ and $d_f=2.1\pm0.3$, respectively. The value for d_b is within the theoretically predicted [27] range of $1 \leqslant d_b \leqslant \min(d_f, 5/3)$ and suggests that the nanotubes behave as rodlike objects, at least at a local length scale, in these nanocomposites. On the other hand, the value of d_f deduced from rheological measurements is in good agreement with those obtained from neutron scattering. These internally consistent scaling of G_p and γ_{critical} with nanotube concentrations indicates that, in fact, the weak and relatively short-range interactions between nanotubes and the multiple pathways between percolating paths dominate the network properties.

For the nanotube hybrids considered here, the strain experienced is nonhomogenous and in particular the strain experienced by a single nanotube inside the network is a function of network size (or tube loading) and different from the bulk strain applied. To accommodate network size effect, a local strain is calculated where bulk strain is modified for dispersed filler effect along the lines adopted by Watanabe *et al.* [28]

$$\gamma_{\text{local}} = [1 + 0.67(\alpha p/100) + 1.62(\alpha p/100)^2]\gamma_{\text{bulk}} \qquad (2)$$

with α being the effective anisotropy of the SWNTs. The value of α used in the determination of local strain was obtained from a fit of the linear dynamic viscosity measure-

ments [15]. Clearly, the local strain used here is reflective of the local stress on the network objects. Under these conditions the stresses that arise from the collective network (i.e., stress contributions from the percolated structures) are neglected in order to calculate the local strain as demonstrated in Eq. (2). Plotting $h(\gamma)$ as a function of local strain [Fig. 4(b)] shows good superpositioning of the data. Considering that the value of $\alpha p/100$ varies from ~ 2 to 6.5 and the relatively low value of p_c, this scaling with local strain [Eq. (2)] is consistent with the development of a somewhat imperfect mastercurve using a rescaled $\gamma_{\text{bulk}}/\gamma_{\text{critical}}$. Finally, the development of time-temperature-concentration-local strain viscoelastic mastercurves with a universal damping function suggests that the linear and non-linear viscoelasticity is dominated by the quiescent state network structure and the local strain experienced by the network elements. Clearly, the addition of nanotubes leads to additional pathways for the interconnection of already formed percolative backbone structures and is directly responsible for the strong scaling of G_p and the large value of the modulus. The onset of shear thinning is accompanied by the removal of these additional pathways of connecting the backbone of the network and not by the breakdown of the backbone of the network. On the other hand, the onset of the failure of the time-strain superposability is perhaps related to the irreversible deformation of the backbone of the fractal network.

Examination of viscoelastic data for an organoclay based nanocomposites with a disordered polystyrene-polyisoprene diblock [18], dominated by short-range interactions, indicates a superpositioning of $h(\gamma)$ with local strain and the onset of shear thinning at a similar value of the local strain ($\gamma_{\text{local}} \sim 0.1$). On the other hand, for the cases of long-range interacting systems such as those observed for a brominated paramethylstyrene-isobutylene polymer with dispersed carbon black [29], aqueous solutions of unmodified clays dispersed in PEO [30] and silica nanoparticles dispersed in PEO [31] such a simple superpositioning fails and is perhaps reflective of the long-range interactions (due to ionic, H-bonding and bridging interactions caused by long-chain polymers bridging between nanoparticles) that dominate those systems.

The authors would like to express their sincere thanks to Venkat Ganesan, Erik Hobbie and Andrew Jackson for useful discussions. This work utilized facilities supported in part by the National Science Foundation under Agreement No. DMR-0454672. We acknowledge the support of the National Institute of Standards and Technology, and the U.S. Department of Commerce, in providing the neutron research facilities used in this work.

[1] E. P. Giannelis, R. Krishnamoorti, and E. Manias, Adv. Polym. Sci. **138**, 107 (1999).
[2] M. Moniruzzaman and K. I. Winey, Macromolecules **39**, 5194 (2006).
[3] R. A. Vaia and E. P. Giannelis, Macromolecules **30**, 7990 (1997).
[4] R. A. Vaia and E. P. Giannelis, MRS Bull. **26**, 394 (2001).
[5] R. Krishnamoorti and K. Yurekli, Curr. Opin. Colloid Interface Sci. **6**, 464 (2001).
[6] J. X. Ren, A. S. Silva, and R. Krishnamoorti, Macromolecules **33**, 3739 (2000).
[7] C. A. Mitchell, J. L. Bahr, S. Arepalli *et al.*, Macromolecules **35**, 8825 (2002).
[8] C. A. Mitchell and R. Krishnamoorti, Macromolecules **40**, 1538 (2007).
[9] M. C. Grant and W. B. Russel, Phys. Rev. E **47**, 2606 (1993).
[10] R. G. Larson, *The Structure and Rheology of Complex Fluids* (Oxford University Press, New York, 1999).
[11] V. Prasad, V. Trappe, A. D. Dinsmore *et al.*, Faraday Discuss. **123**, 1 (2003).
[12] W. H. Shih, W. Y. Shih, S. I. Kim, J. Liu, and I. A. Aksay, Phys. Rev. A **42**, 4772 (1990).
[13] V. Trappe and D. A. Weitz, Phys. Rev. Lett. **85**, 449 (2000).
[14] K. Ninomiya and J. D. Ferry, J. Colloid Sci. **14**, 36 (1959).
[15] T. Chatterjee, K. Yurekli, V. G. Hadjiev *et al.*, Adv. Funct. Mater. **15**, 1832 (2005).
[16] E. K. Hobbie and D. J. Fry, Phys. Rev. Lett. **97**, 036101 (2006).
[17] C. J. Rueb and C. F. Zukoski, J. Rheol. **41**, 197 (1997).
[18] J. X. Ren and R. Krishnamoorti, Macromolecules **36**, 4443 (2003).
[19] L. Berthier, J. Phys.: Condens. Matter **15**, S933 (2003).
[20] P. Sollich, Phys. Rev. E **58**, 738 (1998).
[21] M. Surve, V. Pryamitsyn, and V. Ganesan, Phys. Rev. Lett. **96**, 177805 (2006).
[22] M. Chen and W. B. Russel, J. Colloid Interface Sci. **141**, 564 (1991).
[23] S. Feng, P. N. Sen, B. I. Halperin, and C. J. Lobb, Phys. Rev. B **30**, 5386 (1984).
[24] Y. Kantor and I. Webman, Phys. Rev. Lett. **52**, 1891 (1984).
[25] S. Arbabi and M. Sahimi, Phys. Rev. B **47**, 695 (1993).
[26] M. Sahimi and S. Arbabi, Phys. Rev. B **47**, 703 (1993).
[27] R. de Rooij, D. van den Ende, M. H. G. Duits, and J. Mellema, Phys. Rev. E **49**, 3038 (1994).
[28] Y. Aoki, A. Hatano, T. Tanaka *et al.*, Macromolecules **34**, 3100 (2001).
[29] K. Yurekli, R. Krishnamoorti, M. F. Tse *et al.*, J. Polym. Sci., Part B: Polym. Phys. **39**, 256 (2001).
[30] G. Schmidt, A. I. Nakatani, and C. C. Han, Rheol. Acta **41**, 45 (2002).
[31] Q. Zhang and L. A. Archer, Langmuir **18**, 10435 (2002).
[32] J. G. Barker, C. J. Glinka, J. J. Moyer *et al.*, J. Appl. Crystallogr. **38**, 1004 (2005).